Solid State Communications 138 (2006), 395-398

Multiferroic $TbMnO_3$ nanoparticles

Sharmin Kharrazi[a], Darshan C. Kundaliya[b], S.W. Gosavi[a], S.K. Kulkarni[a]*, T. Venkatesan[b], S.B. Ogale[b], J. Urban[c], S. Park[d] and S.-W. Cheong[d]

[a] DST Unit on Nanoscience, Department of Physics, University of Pune, Ganeshkind, Pune 411 007, India
[b] CSR, University of Maryland, College Park, MD 20742-4111, USA
[c] Department of Inorganic Chemistry, Fritz-Haber-Institut der Max-Planck-Gesellschaft, Faradayweg 4-6, D-14195 Berlin-(Dahlem), Germany
[d] Department of Physics, Rutgers University, Piscataway, NJ 08854, USA
* Corresponding author. Tel.: +91 20 25692678; fax: +91 20 25691684
E-mail address: skk@physics.unipune.ernet.in

Abstract

We report on the synthesis of $TbMnO_3$ nanoparticles by chemical co-precipitation route and their structural, chemical bonding, magnetic and dielectric properties. It is shown that the interesting multiferroic properties of this system as reflected by the concurrent occurrence of magnetic and dielectric transitions are retained in the nanoparticles (size ~40 nm). However, the nanoparticle constitution and properties are seen to depend significantly on the calcination temperature. While the nanoparticles obtained by calcination at 800 °C correspond very well with the reported properties of single phase $TbMnO_3$ (all the key magnetic and dielectric features near 7, 27 and 41 K, albeit with reduced dielectric constant) the nanoparticles obtained by calcination at 900 °C develop a Tb deficient skin which softens the transitions, reducing the dielectric constant further.

Keywords: Multiferroics; Nanostructures; Chemical synthesis

PACS classification codes: 75.30.Sg; 73.61.Tm; 74.25.Ha; 33.60.Fy

1. Introduction

Multiferroics, which represent a class of materials having simultaneous dual property response such as ferromagnetism and ferroelectricity, are under intense investigation at the present time in view of their many projected novel applications and new physics they have to offer [1] and [2]. These materials are being studied either in the form of intrinsic systems involving single phase multiferroic crystalline compounds or in the form of artificially engineered nanostructures comprising of individually non-multiferroic ferromagnetic and ferroelectric components [2], [3], [4], [5], [6], [7], [8], [9], [10] and [11]. Although the recent research on single crystal intrinsic multiferroics has brought out many new phenomena in these materials, these mainly occur at very low temperatures [5], [7], [8], [9], [10] and [11]. Unfortunately, the magneto–electric coupling effects in nanoengineered composites have also been rather weak at practical temperatures [4] and [6]. It is then interesting to explore whether the unique properties of intrinsic multiferroics are retained in their nanoparticle form with possible modifications/enhancements, so that multiferroics themselves can be integrated into nanoengineered configurations with potential beneficial effects. Since, nanoparticles are known to exhibit significant property differences as compared to their bulk counterparts due to their large surface area/volume and related changes in elementary excitations and defect states, it is of interest to explore the corresponding effects in multiferroics. In this work, we report on the synthesis and characterization of $TbMnO_3$ nanoparticles by the chemical co-precipitation route.

We show that the nanoparticles of this compound made from the stoichiometric precursor state retain the interesting multiferroic properties. However, the details are governed by the calcination conditions.

2. Experimental

2.1. Sample preparation

For preparation of $TbMnO_3$ particles, stoichiometric (1:1) amounts of 0.05 M solutions of $TbCl_3 \cdot 6H_2O$ (99.9%, Aldrich) and $MnCl_2 \cdot 4H_2O$ (AR, CDH), in double distilled water, were mixed and stirred for 2 h. This solution of the mixed salts was then; drop wise, added to 0.05 M solution of KOH (AR, RANKEM), under vigorous stirring, leading to a dark brown colour solution. After 17 h stirring at room temperature, the colloidal solution was concentrated using vacuum evaporation. Precipitation was achieved by addition of acetone to the concentrate and removing the supernatant. After drying at room temperature, these samples were calcined (heat treated in air, at atmospheric pressure) at 800 and 900 °C for 90 min.

2.2. Characterization

X-ray diffraction (XRD) data was acquired using SIEMENS-D500 X-ray diffractometer. Fourier transform infrared (FT-IR) spectra were recorded in KBr matrix on a Shimadzu 8400 spectrometer. ESCA LAB-MK II by VG Scientific was used for X-ray photoemission spectroscopy (XPS). High-resolution transmission electron microscopy (HRTEM) using Philips CM 200 FEG microscope has been used to study the microstructure of the particles. The magnetization measurements were carried out using Quantum Design MPMS system.

3. Results and discussion

Fig. 1(a) presents the XRD pattern of a typical 800 °C calcined sample. The average crystallite size calculated using Scherrer formula for these particles is found to be about 40±5 nm. The transmission electron microscopy micrograph shown as in Fig. 1(b) confirms the estimate of particle size based on X-ray diffraction. The peak assignments correspond well to the stoichiometric orthorhombic $TbMnO_3$ phase. FT-IR spectra confirmed the formation of metal–O bond in perovskite structure in case of as prepared sample [12]. Bands between 400 and 600 cm^{-1}, observed in calcined samples (Fig. 1(c)), are due to Tb–O–Mn bending, Tb–O and Mn–O stretching [12] and [13].

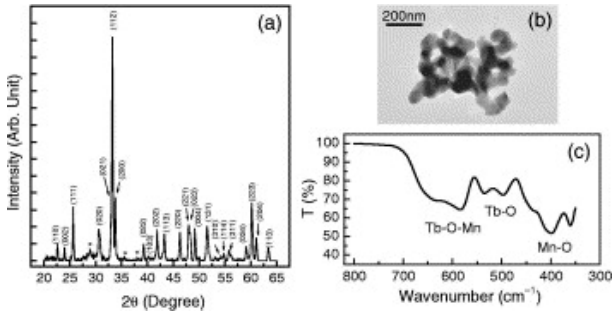

Fig. 1. (a) X-ray diffraction pattern of the 800 °C calcined sample showing orthorhombic $TbMnO_3$ as the major component. A few small impurity peaks are noted in the X-ray data, which could be attributed to phase contributions emanating from a small degree of unintended non-stoichiometry. (b) TEM overview of the nanoparticles and (c) FT-IR spectrum of the same sample.

XPS spectra of the samples showed peaks only due to Tb, Mn, O and small carbon contamination. The Mn 2p peak shape and position were used to decipher the Mn valence state (Mn^{3+} to Mn^{4+} ratio) in the surface region of the nanoparticle (obtained after calcination) which

is accessed by this technique. For this purpose deconvolution of Mn 2p spectra was carried out using XPSPEAK 4.1 software (Fig. 2(a) and (b)). As may be noted, for the 800 °C calcined sample only one component positioned at 641.4 eV corresponding to Mn^{3+} could be fitted and this implies that in this sample the $TbMnO_3$ stoichiometry is maintained almost to the surface suggesting a single phase nanoparticle system. On the other hand a mixture of Mn^{3+} (component at 641.4 eV) and Mn^{4+} (component at 643.5 eV) were noted for the sample calcined at 900 °C. Presence of Mn^{4+} in this sample could be attributed to the formation of a Tb deficient shell on the $TbMnO_3$ core. Indeed a lower relative atomic concentration of Tb with respect to Mn (Tb/Mn=0.8) was noted on the particle surface. The high resolution transmission electron microscopy (HRTEM) shown in Fig. 2(e) clearly brings out the formation of a shell on the surface.

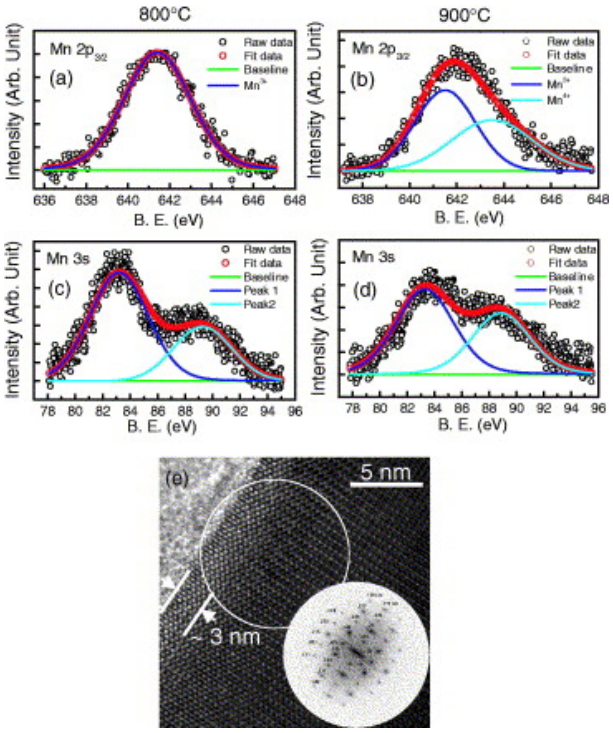

Fig. 2. (a) X-ray photoemission spectroscopy of Mn 2p (upper panels) and Mn 3s (lower panels) peak decomposition of 800 and 900 °C calcined particles (b) HRTEM micrograph of 900 °C calcined particles, showing the presence of the shell.

To further investigate the Mn valence state in the samples, deconvolution of Mn 3s spectra was carried out. Mn 3s core level exhibits an exchange splitting with a magnitude depending on the interaction of Mn 3s and Mn 3d electrons. Since, the number of electrons in d level is more in Mn^{3+}, therefore, exchange interaction between s and d electrons is stronger. This leads to splitting of Mn3s spectrum which would be more in Mn^{3+} than in Mn^{4+} [14], [15] and [16]. Here, XPSPEAK 4.1 has been again applied for the peak deconvolution. Fig. 2(c) and (d) (lower panels) show the Mn 3s components due to 3s core level splitting in samples. The second component is fitted as a convolution of components due to contribution of Mn^{3+} and Mn^{4+} ions. Therefore, position of the second peak is an indirect measure of relative presence of Mn^{3+} and Mn^{4+} ions in the sample. The splitting magnitudes in the 800 °C calcined and 900 °C calcined samples were found to be ~6.1 and ~5.5 eV, respectively. The highest Mn 3s splitting along with no Mn^{4+} in Mn $2p_{3/2}$ spectrum for the sample calcined at 800 °C are in excellent mutual agreement and imply the absence of any surface shell in this sample. The lowering of the

splitting in the 900 °C calcined sample further supports the formation of a Tb deficient surface shell in this sample.

The temperature profile of the magnetization (M) for 800 °C calcined particles (Fig. 3(a), upper panel) shows well defined features near ~40 and ~7 K, close to those observed in single crystalline $TbMnO_3$ corresponding to the sine wave ordering of Mn^{3+} moments and magnetic ordering of Tb^{3+} moments, respectively. The feature near ~27 K observed in single crystal $TbMnO_3$ and attributed to the incommensurate–commensurate (or lock-in) transition does not appear to be strong in the nanoparticle case. However, its presence is reflected in the derivative curve in Fig. 3(a) (middle panel). It is possible that the lock-in transition is softened in nanoparticles due to intrinsic strain gradients, especially since this particular transition is related to a longer length scale. The observation of all the expected transitions further establishes the presence of stoichiometric crystalline $TbMnO_3$ in these particles obtained by calcination at 800 °C. In the sample of the 900 °C calcined case the measurement at 50 Oe did not reveal any significant features, however, the measurement at higher field (5 T) brought out feeble signatures at ~27 and ~7 K in the derivative curve (Fig. 3(b), middle panel) with just a hint of the feature near 41 K (which only shows up in the second derivative).

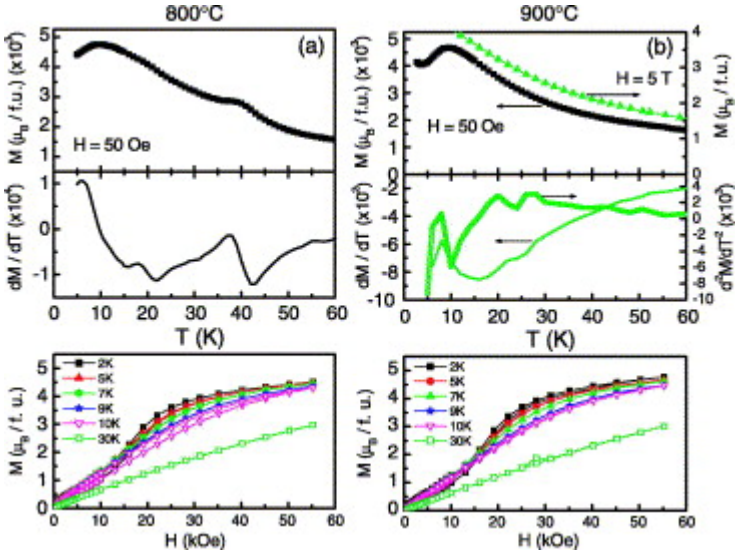

Fig. 3. Upper panel shows zero field cooled temperature (*T*) dependent magnetization (*M*) plot for 800 and 900 °C calcined particles with applied magnetic field of 0.005 and 5 T. Middle panel shows first derivative of the zero field cooled magnetization with respect to *T* for 800 °C and first and second derivatives for 900 °C calcined sample. Lower panels show magnetization (*M*) vs. applied magnetic field (*H*) isotherms at various temperatures for the calcined particles.

Further, the magnetization (*M*) vs. applied magnetic field (*H*) isotherms of the calcined particles (Fig. 3 lower panels) showed behavior broadly similar to the bulk but modified in details. At 30 K a paramagnetic behavior could be observed and the same continued down to about 10 K. As the temperature decreased, further down, an upturn step in the magnetization curve began to appear near 1.5 T, which became clearer and sharper with further decrease in temperature below ~7 K. This metamagnetic feature [17], [18] and [19] has been briefly discussed by Troyanchuk et al. [20] for the $TbMnO_{3.01}$ case and has been correlated with the magnetic ordering of Tb ions since it occurs near and below the ordering temperature for Tb moments. The precise understanding of the mode and nature of coupling of the spin order on the Tb and Mn sublattices, and the corresponding consequences for the para-ferro (or rather canted antiferro) type metamagnetic transition clearly needs further work on bulk crystalline materials. Quezel et al. have discussed the magnetization of $TbMnO_3$ at 1.5 K as a function of applied magnetic field *H* [21]. When *H* is along *a*-axis the magnetization gets saturated near ~20 kOe and when it is along

b-axis, a jump is noted near ~50 kOe. For *H* along *c*-axis the behavior is linear. In our case, since we have random orientation of the particles with reference to field, the combination of the magnetization curves along *a* and *b* axes should lead to the apparent shift of the jump to lower field as observed by us.

Finally, we show in Fig. 4 the temperature dependence of dielectric constant for the nanoparticles obtained by calcinations at 800 and 900 °C. Broadly speaking the behavior reflects an upward rise in ε near 41 K, a flattening below 27 K and lowering near 7 K. This behavior is primarily of the type that is shown to occur in single crystal $TbMnO_3$ when the polarizing field is applied parallel to the *a*-axis. The dielectric constant in bulk crystal is shown to exhibit a sharp peak near 27 K, which is seen to be tiny in our data on nanoparticles, although seen somewhat more clearly in the 900 °C calcined particles. The weakness of this peak corresponds to the observed weakness of the corresponding magnetic anomaly near 27 K. However, the significant fact that all these dielectric features occur at the same temperatures at which the magnetic transitions are also observed implies that the key multiferroic property is retained by the nanoparticles. It may further be noted that the dielectric constant value in 800 °C calcined case is lower than that for bulk single crystal $TbMnO_3$, but is clearly much higher than that for 900 °C calcined case, which leads to nanoparticles with a Tb deficient surface shell. It may be recalled that in this latter case of 900 °C calcined powders the magnetic transitions were also seen to have been softened. We believe that the lowering of dielectric constant in 800 °C single phase nanoparticles with respect to the single crystal case may be due to slight non-stoichiometry, disorder or some contribution of particle size effect on dielectric response. Further lowering of dielectric constant and softening of the magnetic transitions in the 900 °C calcined system could be attributed to the effects of the Tb deficient surface shell, and its coupling with and control of the dielectric and magnetic response of the $TbMnO_3$ core.

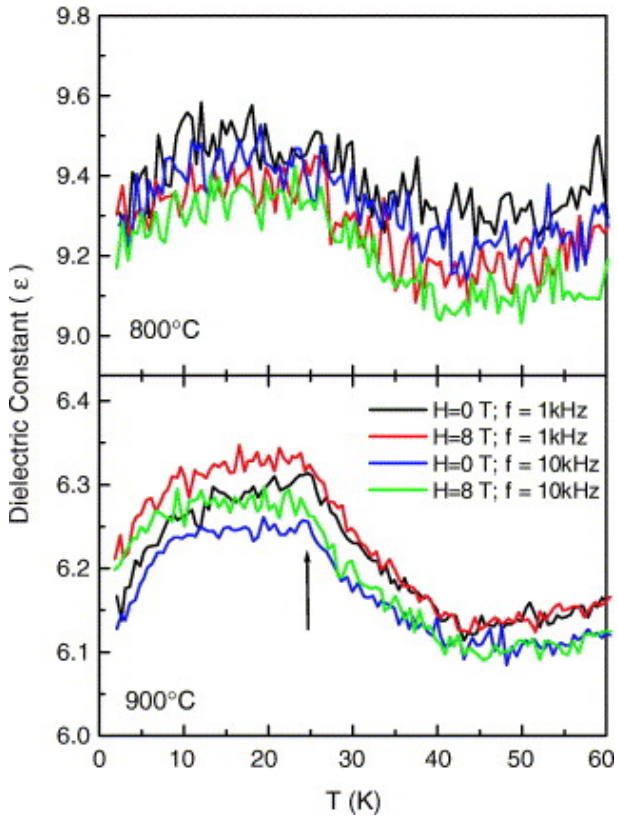

Fig. 4. Temperature dependent dielectric constant ε, in different frequency range, with an applied magnetic field of 0 and 8 T. The applied electric field direction is perpendicular to the external magnetic field.

4. Conclusions

In conclusion, we have shown that by using chemical co-precipitation route it is possible to synthesize nearly single phase $TbMnO_3$ nanoparticles (calcination at 800 °C), which retain the interesting multiferroic response reflecting the coupling of the magnetic and dielectric transitions. It is shown that calcination process controls the nanoparticle constitution and affects the properties significantly. In particular, calcination at higher temperature (900 °C) leads to nanoparticles with a Tb deficient surface shell.

Acknowledgements

This work has been funded by DST, India. SKK and SK acknowledge the support by UGC, India. The work at Maryland and Rutgers was supported under NSF-MRSEC grant # DMR-0520471.

References

[1] N.A. Hill, *Annu. Rev. Mater. Res.* **32** (2002), p. 1.

[2] M. Fiebig, *J. Phys. D: Appl. Phys.* **38** (2005), p. R123.

[3] W. Prellier, M.P. Singh and P. Murugavel, *J. Phys.: Condens. Matter* **17** (2005), p. R803.

[4] J. Wang, J.B. Neaton, H. Zheng, V. Nagarajan, S.B. Ogale, B. Liu, D. Viehland, V. Vaithyanathan, D.G. Schlom, U.V. Waghmare, N.A. Spaldin, K.M. Rabe, M. Wuttig and R. Ramesh, *Science* **299** (2003), p. 1719.

[5] T. Kimura, T. Goto, H. Shintani, K. Ishizaka, T. Arima and Y. Tokura, *Nature* **426** (2003), p. 55.

[6] H. Zheng, J. Wang, S.E. Lofland, Z. Ma, L. Mohaddes-Ardabili, T. Zhao, L. Salaanca-Riba, S.R. Shinde, S.B. Ogale, F. Bai, D. Viehland, Y. Jia, D.G. Schlom, M. Wutting, A. Roytburd and R. Ramesh, *Science* **303** (2004), p. 661.

[7] N. Hur, S. Park, P.A. Sharma, J.S. Ahn, S. Guha and S.-W. Cheong, *Nature* **429** (2004), p. 392.

[8] Y. Ogawa, Y. Kaneko, J.P. He, X.Z. Yu, T. Arima and Y. Tokura, *Phys. Rev. Lett.* **92** (2004), p. 047401.

[9] M. Kubota, T. Arima, Y. Kaneko, J.P. He, X.Z. Yu and Y. Tokura, *Phys. Rev. Lett.* **92** (2004), p. 137401.

[10] J.H. Jung, M. Matsubara, T. Arima, J.P. He, Y. Kaneko and Y. Tokura, *Phys. Rev. Lett.* **93** (2004), p. 037403.

[11] D.C. Kundaliya, S.B. Ogale, S. Dhar, K.F. McDonald, E. Knoesel, T. Osedach, S.E. Lofland, S.R. Shinde and T. Venkatesan, *J. Magn. Magn. Mater.* **299** (2006), p. 307.

[12] C. Bernard, B. Durand, M. Verelst and P. Lecante, *J. Mater. Sci.* **39** (2004), p. 2821.

[13] S. Mathur, H. Shen and J. Sol–Gel, *Sci. Technol.* **25** (2002), p. 147.

[14] T. Saitoh, A.E. Bocquet, T. Mizokawa, H. Namatame, A. Fujimori, M. Abbate, Y. Takeda and M. Takano, *Phys. Rev. B* **51** (1995), p. 13942.

[15] M. Oku, K. Hirokawa and S. Ikeda, *J. El. Spectr. Rel. Phen.* **7** (1975), p. 465.

[16] I.N. Shabanova and N.V. Keller, *Surf. Interface Anal.* **32** (2001), p. 114.

[17] J.L. Luo, N.L. Wang, G.T. Liu, D. Wu, X.N. Jing, F. Hu and T. Xiang, *Phys. Rev. Lett.* **93** (2004), p. 187203.

[18] T. Kimura, G. Lawes and A.P. Ramirez, *Phys. Rev. Lett.* **94** (2005), p. 137201.

[19] H. Ueda, H.A. Katori, H. Mitamura, T. Goto and H. Takagi, *Phys. Rev. Lett.* **94** (2005), p. 047202.

[20] O.Ya. Troyanchuk, N.V. Kasper, H. Szymczak and A. Nabialek, *Low Temp. Phys.* **23** (1997), p. 300.

[21] S. Quezel, F. Tcheou, J. Rossat-ignod, G. Quezel and E. Roudaut, *Physica B+C* **86–88** (1977), p. 916